EUROPEAN ORGANIZATION FOR NUCLEAR RESEARCH

CERN–PH–EP/2009–011
4 June 2009

Measurement of the Longitudinal Spin Transfer to Λ and $\bar{\Lambda}$ Hyperons in Polarised Muon DIS

COMPASS Collaboration

Abstract

The longitudinal polarisation transfer from muons to Λ and $\bar{\Lambda}$ hyperons, $D_{LL}^{\Lambda(\bar{\Lambda})}$, has been studied in deep inelastic scattering off an unpolarised isoscalar target at the COMPASS experiment at CERN. The spin transfers to Λ and $\bar{\Lambda}$ produced in the current fragmentation region exhibit different behaviours as a function of x and x_F. The measured x and x_F dependences of D_{LL}^{Λ} are compatible with zero, while $D_{LL}^{\bar{\Lambda}}$ tends to increase with x_F, reaching values of 0.4 - 0.5. The resulting average values are $D_{LL}^{\Lambda} = -0.012 \pm 0.047 \pm 0.024$ and $D_{LL}^{\bar{\Lambda}} = 0.249 \pm 0.056 \pm 0.049$. These results are discussed in the frame of recent model calculations.

PACS: 13.60.Rj, 13.87.Fh, 13.88.+e, 14.20.Jn
Keywords: lepton deep inelastic scattering, strange particles, polarisation, spin transfer, hyperons

submitted to the European Physical Journal C

COMPASS Collaboration

M. Alekseev[30], V.Yu. Alexakhin[8], Yu. Alexandrov[16], G.D. Alexeev[8], A. Amoroso[28], A. Austregesilo[11,18], B. Badełek[31], F. Balestra[28], J. Ball[23], J. Barth[4], G. Baum[1], Y. Bedfer[23], J. Bernhard[14], R. Bertini[28], M. Bettinelli[17], R. Birsa[25], J. Bisplinghoff[3], P. Bordalo[13,a], F. Bradamante[26], A. Bravar[25], A. Bressan[26], G. Brona[31], E. Burtin[23], M.P. Bussa[28], A. Chapiro[27], M. Chiosso[28], S.U. Chung[18], A. Cicuttin[25,27], M. Colantoni[29], M.L. Crespo[25,27], S. Dalla Torre[25], T. Dafni[23], S. Das[7], S.S. Dasgupta[6], O.Yu. Denisov[29,b], L. Dhara[7], V. Diaz[25,27], A.M. Dinkelbach[18], S.V. Donskov[22], N. Doshita[2,33], V. Duic[26], W. Dünnweber[17], A. Efremov[8], P.D. Eversheim[3], W. Eyrich[9], M. Faessler[17], A. Ferrero[28,11], M. Finger[20], M. Finger jr.[8], H. Fischer[10], C. Franco[13], J.M. Friedrich[18], R. Garfagnini[28], F. Gautheron[1], O.P. Gavrichtchouk[8], R. Gazda[31], S. Gerassimov[16,18], R. Geyer[17], M. Giorgi[26], B. Gobbo[25], S. Goertz[2,4], S. Grabmüller[18], O.A. Grajek[31], A. Grasso[28], B. Grube[18], R. Gushterski[8], A. Guskov[8], F. Haas[18], D. von Harrach[14], T. Hasegawa[15], J. Heckmann[2], F.H. Heinsius[10], M. Hermann[3], R. Hermann[14], F. Herrmann[10], C. Heß[2], F. Hinterberger[3], N. Horikawa[19,c], Ch. Höppner[18], N. d'Hose[23], C. Ilgner[11,17], S. Ishimoto[19,d], O. Ivanov[8], Yu. Ivanshin[8], B. Iven[3], T. Iwata[33], R. Jahn[3], P. Jasinski[14], G. Jegou[23], R. Joosten[3], E. Kabuß[14], D. Kang[10], B. Ketzer[18], G.V. Khaustov[22], Yu.A. Khokhlov[22], Yu. Kisselev[1,2], F. Klein[4], K. Klimaszewski[31], S. Koblitz[14], J.H. Koivuniemi[2], V.N. Kolosov[22], E.V. Komissarov[8,+], K. Kondo[2,33], K. Königsmann[10], R. Konopka[18], I. Konorov[16,18], V.F. Konstantinov[22], A. Korzenev[14,b], A.M. Kotzinian[8], O. Kouznetsov[8,23], K. Kowalik[31,23], M. Krämer[18], A. Kral[21], Z.V. Kroumchtein[8], R. Kuhn[18], F. Kunne[23], K. Kurek[31], J.M. Le Goff[23], A.A. Lednev[22], A. Lehmann[9], S. Levorato[26], J. Lichtenstadt[24], T. Liska[21], A. Maggiora[29], M. Maggiora[28], A. Magnon[23], G.K. Mallot[11], A. Mann[18], C. Marchand[23], J. Marroncle[23], A. Martin[26], J. Marzec[32], F. Massmann[3], T. Matsuda[15], A.N. Maximov[8,+], W. Meyer[2], T. Michigami[33], Yu.V. Mikhailov[22], M.A. Moinester[24], A. Mutter[10,14], A. Nagaytsev[8], T. Nagel[18], J. Nassalski[31], S. Negrini[3], F. Nerling[10], S. Neubert[18], D. Neyret[23], V.I. Nikolaenko[22], A.G. Olshevsky[8], M. Ostrick[4,14], A. Padee[32], R. Panknin[4], D. Panzieri[30], B. Parsamyan[28], S. Paul[18], B. Pawlukiewicz-Kaminska[31], E. Perevalova[8], G. Pesaro[26], D.V. Peshekhonov[8], G. Piragino[28], S. Platchkov[23], J. Pochodzalla[14], J. Polak[12,26], V.A. Polyakov[22], G. Pontecorvo[8], J. Pretz[4], C. Quintans[13], J.-F. Rajotte[17], S. Ramos[13,a], V. Rapatsky[8], G. Reicherz[2], D. Reggiani[11], A. Richter[9], F. Robinet[23], E. Rocco[28], E. Rondio[31], D.I. Ryabchikov[22], V.D. Samoylenko[22], A. Sandacz[31], H. Santos[13,a], M.G. Sapozhnikov[8], S. Sarkar[7], G. Sbrizzai[26], P. Schiavon[26], C. Schill[10], L. Schmitt[18,e], W. Schröder[9], O.Yu. Shevchenko[8], H.-W. Siebert[14], L. Silva[13], L. Sinha[7], A.N. Sissakian[8], M. Slunecka[8], G.I. Smirnov[8], S. Sosio[28], F. Sozzi[26], A. Srnka[5], M. Stolarski[31,11], M. Sulc[12], R. Sulej[32], S. Takekawa[26], S. Tessaro[25], F. Tessarotto[25], A. Teufel[9], L.G. Tkatchev[8], G. Venugopal[3], M. Virius[21], N.V. Vlassov[8], A. Vossen[10], Q. Weitzel[18], R. Windmolders[4], W. Wiślicki[31], H. Wollny[10], K. Zaremba[32], E. Zemlyanichkina[8], M. Ziembicki[32], J. Zhao[14,25], N. Zhuravlev[8] and A. Zvyagin[17]

[1] Universität Bielefeld, Fakultät für Physik, 33501 Bielefeld, Germany[f]
[2] Universität Bochum, Institut für Experimentalphysik, 44780 Bochum, Germany[f]
[3] Universität Bonn, Helmholtz-Institut für Strahlen- und Kernphysik, 53115 Bonn, Germany[f]
[4] Universität Bonn, Physikalisches Institut, 53115 Bonn, Germany[f]
[5] Institute of Scientific Instruments, AS CR, 61264 Brno, Czech Republic[g]
[6] Burdwan University, Burdwan 713104, India[h]
[7] Matrivani Institute of Experimental Research & Education, Calcutta-700 030, India[i]
[8] Joint Institute for Nuclear Research, 141980 Dubna, Moscow region, Russia
[9] Universität Erlangen–Nürnberg, Physikalisches Institut, 91054 Erlangen, Germany[f]
[10] Universität Freiburg, Physikalisches Institut, 79104 Freiburg, Germany[f]
[11] CERN, 1211 Geneva 23, Switzerland
[12] Technical University in Liberec, 46117 Liberec, Czech Republic[g]
[13] LIP, 1000-149 Lisbon, Portugal[j]
[14] Universität Mainz, Institut für Kernphysik, 55099 Mainz, Germany[f]
[15] University of Miyazaki, Miyazaki 889-2192, Japan[k]
[16] Lebedev Physical Institute, 119991 Moscow, Russia
[17] Ludwig-Maximilians-Universität München, Department für Physik, 80799 Munich, Germany[f,l]
[18] Technische Universität München, Physik Department, 85748 Garching, Germany[f,l]
[19] Nagoya University, 464 Nagoya, Japan[k]
[20] Charles University, Faculty of Mathematics and Physics, 18000 Prague, Czech Republic[g]
[21] Czech Technical University in Prague, 16636 Prague, Czech Republic[g]
[22] State Research Center of the Russian Federation, Institute for High Energy Physics, 142281 Protvino, Russia
[23] CEA DAPNIA/SPhN Saclay, 91191 Gif-sur-Yvette, France
[24] Tel Aviv University, School of Physics and Astronomy, 69978 Tel Aviv, Israel[m]
[25] Trieste Section of INFN, 34127 Trieste, Italy
[26] University of Trieste, Department of Physics and Trieste Section of INFN, 34127 Trieste, Italy
[27] Abdus Salam ICTP and Trieste Section of INFN, 34127 Trieste, Italy
[28] University of Turin, Department of Physics and Torino Section of INFN, 10125 Turin, Italy
[29] Torino Section of INFN, 10125 Turin, Italy
[30] University of Eastern Piedmont, 1500 Alessandria, and Torino Section of INFN, 10125 Turin, Italy
[31] Sołtan Institute for Nuclear Studies and University of Warsaw, 00-681 Warsaw, Poland[n]
[32] Warsaw University of Technology, Institute of Radioelectronics, 00-665 Warsaw, Poland[o]
[33] Yamagata University, Yamagata, 992-8510 Japan[k]
[+] Deceased
[a] Also at IST, Universidade Técnica de Lisboa, Lisbon, Portugal
[b] On leave of absence from JINR Dubna
[c] Also at Chubu University, Kasugai, Aichi, 487-8501 Japan[j]
[d] Also at KEK, 1-1 Oho, Tsukuba, Ibaraki, 305-0801 Japan
[e] Also at GSI mbH, Planckstr. 1, D-64291 Darmstadt, Germany
[f] Supported by the German Bundesministerium für Bildung und Forschung
[g] Suppported by Czech Republic MEYS grants ME492 and LA242
[h] Supported by DST-FIST II grants, Govt. of India
[i] Supported by the Shailabala Biswas Education Trust
[j] Supported by the Portuguese FCT - Fundação para a Ciência e Tecnologia grants POCTI/FNU/49501/2002 and POCTI/FNU/50192/2003
[k] Supported by the MEXT and the JSPS under the Grants No.18002006, No.20540299 and No.18540281; Daiko Foundation and Yamada Foundation
[l] Supported by the DFG cluster of excellence 'Origin and Structure of the Universe' (www.universe-cluster.de)
[m] Supported by the Israel Science Foundation, founded by the Israel Academy of Sciences and Humanities
[n] Supported by Ministry of Science and Higher Education grant 41/N-CERN/2007/0
[o] Supported by KBN grant nr 134/E-365/SPUB-M/CERN/P-03/DZ299/2000

1 Introduction

The study of the Λ and $\bar{\Lambda}$ hyperon polarisation in DIS is important for the understanding of the nucleon structure, the mechanisms of hyperon production and the hyperon spin structure. In particular, it may provide valuable information on the unpolarised strange quark distributions $s(x)$ and $\bar{s}(x)$ in the nucleon. In this paper measurements of the longitudinal polarisation of Λ and $\bar{\Lambda}$ hyperons produced in deep-inelastic scattering (DIS) of polarised muons off an unpolarised isoscalar target are presented.

In a simple parton model a polarised lepton interacts preferentially with a quark carrying a specific spin orientation. After the absorption of the hard virtual photon the remaining system consists of the scattered quark and the target remnant which are both polarised. During the hadronisation, part of the polarisation of the scattered quark or the target remnant is transferred to the produced hyperon. Therefore, the value of hyperon polarisation will depend on the spin dynamics in the hadronisation not only of the scattered quarks, but also of the target remnant. For the kinematic conditions of the COMPASS experiment the role of these effects has been considered in [1]. It occurs that even in the current fragmentation region the spin transfer from the polarised target remnant to the Λ hyperon is substantial. The situation is different for the spin transfer to $\bar{\Lambda}$. A recent analysis [2] shows that at the energy of the COMPASS experiment the $\bar{\Lambda}$ polarisation is dominated by the spin transfer from the $\bar{s}$-quarks, and hence is sensitive to the $\bar{s}(x)$ distribution in the nucleon.

The polarisation of the produced hyperons depends also on their spin structure. For example, in the SU(6) quark model the whole spin of the Λ is carried by the s-quark. Therefore, under the assumption of the quark helicity conservation, even if the struck u- or d-quark were completely polarised this would not lead to a polarisation of the Λ hyperon. As a consequence, if the dominant mechanism of Λ production is the independent u- and d-quark fragmentation, then the polarisation of the directly produced Λ hyperons should be $P_\Lambda \sim 0$.

Using $\mathrm{SU(3)_f}$ symmetry and experimental data for spin-dependent quark distributions in the proton, the authors of [3] predict that the contributions of u- and d-quarks to the Λ spin are negative and substantial, at the level of 20% for each light quark. In this model the spin transfer from u- or d-quarks would lead to a negative spin transfer to Λ.

The Λ and $\bar{\Lambda}$ hyperons can also be produced indirectly, via decays of heavy hyperons such as $\Sigma^0, \Sigma(1385), \Xi$ etc. In this case a non-zero spin transfer from u- and d-quarks to Λ is also possible [4],[5].

The spin transfer to Λ and $\bar{\Lambda}$ hyperons has been studied extensively in a number of theoretical models [6, 7, 8, 9, 10, 11, 12, 13, 14] for e^+e^- collisions and lepton DIS. From a theoretical point of view the simplest case is the polarisation of the hyperons formed in e^+e^- annihilation at the Z-peak, where hadronisation of the $q\bar{q}$-system can be well described using independent fragmentation. The electroweak theory predicts for the s-quarks from Z decay a longitudinal polarisation of -0.94. The corresponding antiquarks have the same degree of polarisation, but with opposite helicity. The fraction of this polarisation that is transferred to the produced $\Lambda(\bar{\Lambda})$ hyperon was studied using e^+e^- annihilation by ALEPH [15] and OPAL [16] experiments at LEP. Both experiments find large and negative values for the hyperon longitudinal polarisation, with a strong dependence on the fraction of the primary quark momentum carried by the hyperon. These results clearly indicate that the fragmentation processes preserve a strong correlation between the fragmenting quark helicity and the final hyperon polarisation. However, as was shown in [8], these data are insufficient to distinguish between predictions of the SU(6) or the BJ [3] models.

The longitudinal spin transfer to $\Lambda(\bar{\Lambda})$ in DIS was measured in a number of experiments [17, 18, 19, 20, 21, 22, 23, 24]. The earlier neutrino DIS experiments [17, 18, 19] have found an indication for a large negative polarisation of Λ hyperons formed in the target fragmentation region. However, the statistics of each of these experiments does not exceed 500 events. The E665 Collaboration [22] has measured $\Lambda(\bar{\Lambda})$ production using 470 GeV positive muons scattered off hydrogen, deuterium and other nuclear targets. The total number of events amounts to 750 Λ and 650 $\bar{\Lambda}$. The spin transfers of Λ and $\bar{\Lambda}$ hyperons were found to have opposite signs: negative for Λ and positive for $\bar{\Lambda}$. The NOMAD Collaboration [20, 21] has studied Λ and $\bar{\Lambda}$ polarisation in DIS using 43 GeV muon neutrinos. The total number of events amounts to 8087 Λ, mainly in the target fragmentation region, and 649 $\bar{\Lambda}$. The results confirm those of earlier experiments [17, 18, 19] and show a large negative longitudinal polarisation P_Λ in the target fragmentation region while no significant spin transfer to Λ was detected in the current fragmentation region. This region was later explored by the HERMES Collaboration [23]. The Λ polarisation was measured using the 27.6 GeV longitudinally polarised positron beam. The total statistics is 7300 Λ. Within the experimental uncertainties, the resulting spin transfer was found to be compatible with zero. The STAR Collaboration at RHIC [24] has measured the longitudinal spin transfer to Λ and $\bar{\Lambda}$ in polarised proton-proton collisions at a centre of mass energy $\sqrt{s} = 200$ GeV. The data sample comprises 30000 Λ and 24000 $\bar{\Lambda}$. The measurement is limited to the mid-rapidity region ($|\eta| < 1$) with an average

$x_F = 7.5 \cdot 10^{-3}$. (The Feynman variable is $x_F = 2p_L/W$, where p_L is the particle longitudinal momentum in the hadronic centre-of-mass system, whose invariant mass is W.) A small spin transfer, compatible with zero, was found for both Λ and $\bar{\Lambda}$.

The statistical accuracy achieved in the measurements discussed above is quite limited, particularly, in the current fragmentation region. The data on the polarisation of the Λ hyperons tend to be compatible with zero and no clear conclusions about the spin transfer mechanism can be drawn. The dependence of the spin transfer on the Bjorken scaling variable x and x_F has been mapped out by the HERMES experiment [23], but for the Λ hyperon only.

The present analysis is based on about 70000 Λ and 42000 $\bar{\Lambda}$ events. Our data allow to explore the x-dependence of the spin transfer to Λ in a large x-interval and to measure, for the first time, the x- and x_F-dependences of the spin transfer to $\bar{\Lambda}$. A substantial $\bar{\Lambda}$ polarisation is found, which is important for the investigation of the strange quark distribution in the nucleon.

2 Data analysis

We have studied Λ and $\bar{\Lambda}$ production by scattering 160 GeV polarised μ^+ off a polarised ^{6}LiD target in the COMPASS experiment (NA58) at CERN. A detailed description of the COMPASS experimental setup is given elsewhere [25].

The data used in the present analysis were collected during the years 2003–2004. The longitudinally polarised muon beam has an average polarisation of $P_b = -0.76 \pm 0.04$ in the 2003 run and of $P_b = -0.80 \pm 0.04$ in the 2004 run. The momentum of each beam muon is measured upstream of the experimental area in a beam momentum station consisting of several planes of scintillator strips or scintillating fibres with a dipole magnet in between. The target consists of two 60 cm long, oppositely polarised cells. The data from both longitudinal target spin orientations were recorded simultaneously and averaged in the present analysis. The number of events with $\Lambda(\bar{\Lambda})$ hyperons for each target spin orientation is the same within 1% accuracy.

The event selection requires a reconstructed interaction vertex defined by the incoming and the scattered muon located inside the target. DIS events are selected by cuts on the photon virtuality ($Q^2 > 1$ $(\mathrm{GeV}/c)^2$) and on the fractional energy of the virtual photon ($0.2 < y < 0.9$). The data sample consists of $8.67 \cdot 10^7$ DIS events from the 2003 run and $22.5 \cdot 10^7$ DIS events from the 2004 run.

The Λ and $\bar{\Lambda}$ hyperons are identified by their decays into $p\pi^-$ and $\bar{p}\pi^+$. To estimate systematic effects, decays of $K^0_S \to \pi^+\pi^-$ are also analysed. Events with Λ, $\bar{\Lambda}$ and $\mathrm{K^0_S}$ decays are selected by demanding that two hadron tracks form a secondary vertex. Particle identification provided by a ring imaging Cherenkov detector and calorimeters is not used for hadrons in the present analysis. The results of the analysis for RICH-identified hadrons will be the subject of a separate paper with larger statistics. In order to suppress background events, the secondary vertex is required to be within a 105 cm long fiducial region starting 5 cm downstream of the target. The angle θ_{col} between the hyperon momentum and the line connecting the primary and the secondary vertex is required to be $\theta_{col} < 0.01$ rad. This cut selects events with the correct direction of the hyperon momentum vector with respect to the primary vertex, which results in a reduction of the combinatorial background. A cut on the transverse momentum p_t of the decay products with respect to the hyperon direction of $p_t > 23$ MeV/c is applied to reject e^+e^- pairs due to γ conversion. Only particles with momenta larger than 1 GeV/c were selected to provide optimal tracking efficiency.

The $p\pi^-$ and $\bar{p}\pi^+$ invariant mass distributions with peaks of Λ and $\bar{\Lambda}$ are shown in Fig. 1 for the data of the 2004 run. The main sources of background are events from $\mathrm{K^0_S}$ decays and combinatorial background. A Monte Carlo (MC) simulation shows that the percentage of kaon background changes from 1 to 20 %, when $\cos\theta$ varies from -1 to 1, where θ is the angle between the direction of the decay proton(antiproton) in the $\Lambda(\bar{\Lambda})$ rest frame and the quantisation axis along the momentum vector of the virtual photon. At small and negative values of $\cos\theta$ the invariant mass distribution of the kaon background is flat. However, at $\cos\theta \sim 1$, the kaon contribution is concentrated mainly at small values of the invariant mass on the left side of the $\Lambda(\bar{\Lambda})$ peak in Fig. 1. In this angular region the distribution of the kaon events under the $\Lambda(\bar{\Lambda})$ peak changes rapidly. In order to minimise the influence of the kaon background, the angular interval was limited to $-1 < \cos\theta < 0.6$ (a similar cut was introduced in the analysis of the STAR data [24]). This cut reduces the $\Lambda(\bar{\Lambda})$ signal by $\sim$10%.

The total number of events after all selection cuts is $N(\Lambda) = 69500 \pm 360$, $N(\bar{\Lambda}) = 41600 \pm 310$ and $N(K^0_S) = 496000 \pm 830$. The large amount of $\bar{\Lambda}$ events is a unique feature of the COMPASS experiment.

3 Experimental results

The distributions of experimental and MC events satisfying the selection cuts are shown in Fig. 2 for Λ and $\bar{\Lambda}$ as functions of different kinematic variables for events of the 2004 run. The data from

the 2003 run have similar distributions. Both experimental and MC distributions are normalised on the total number of events. The acceptance of the COMPASS spectrometer selects $\Lambda(\bar{\Lambda})$ only in the current fragmentation region. For this analysis we take $\Lambda(\bar{\Lambda})$ events in the interval $0.05 < x_F < 0.5$ with the average value $\bar{x}_F = 0.22$ (0.20). In contrast to other DIS experiments [20, 21, 22, 23], our data cover a large region of Bjorken x ($\bar{x} = 0.03$) extending to values of x as low as $x = 0.005$. The average value of Λ fractional energy is $\bar{z} = 0.27$. The average values of y and Q^2 are 0.46 and 3.7 $(\mathrm{GeV/c})^2$, respectively.

The distributions of the kinematic variables for $\bar{\Lambda}$ produced in DIS differ from the Λ ones, since $\bar{\Lambda}$ production is suppressed in the target fragmentation region. However, in the current fragmentation region the $\bar{\Lambda}$ have practically the same kinematic distributions as the Λ (see Fig. 2).

The shaded histograms in Fig. 2 show the same distributions for MC events. The COMPASS Monte Carlo code is based on the LEPTO 6.5.1 generator [26] providing DIS events which are passed through a GEANT-based apparatus simulation programme and the same chain of reconstruction procedures as the experimental events. To provide better agreement between data and MC, a tuning of several LEPTO (JETSET) parameters has been performed. The values of the modified parameters are compared with the default ones [27] and with those used in previous experiments in Table 1. Here, the PARJ(21) parameter corresponds to the width of the Gaussian transverse momentum distribution for the primary hadrons. The parameters PARJ(23), PARJ(24) are used to add non-Gaussian tails to the transverse momentum distribution, PARJ(41), PARJ(42) are the parameters of the symmetric Lund fragmentation function [27].

Table 1: Comparison of the default [27] and modified JETSET parameters. Corresponding values used in the HERMES [23] and NOMAD [20] experiments are also given.

Parameters	Default	Used	HERMES	NOMAD
PARJ(21)	0.36	0.4	0.38	0.41
PARJ(23)	0.01	0.08	0.03	0.15
PARJ(24)	2.0	2.5	2.5	2.0
PARJ(41)	0.3	0.95	1.13	1.5
PARJ(42)	0.58	0.37	0.37	0.9

Some small but systematic differences were observed between the momentum spectra seen in the data and those given by the MC simulation. To overcome these differences, the reconstructed MC events are weighted in order to provide the same momentum and z distributions as the data. The weighting of the MC events leads to a slight modification of the angular acceptance, which is below 2 % in the whole angular range.

3.1 Determination of the angular distributions

The acceptance corrected angular distribution of the decay protons(antiprotons) in the $\Lambda(\bar{\Lambda})$ rest frame is

$$\frac{1}{N_{tot}} \cdot \frac{dN}{d\cos\theta} = \frac{1}{2} \cdot (1 + \alpha P_L \cos\theta). \tag{1}$$

Here, N_{tot} is the total number of acceptance corrected $\Lambda(\bar{\Lambda})$, the longitudinal polarisation P_L is the projection of the polarisation vector on the momentum vector of the virtual photon, $\alpha = +(-)0.642 \pm 0.013$ is the $\Lambda(\bar{\Lambda})$ decay parameter, θ is the angle between the direction of the decay proton for Λ (antiproton - for $\bar{\Lambda}$, positive π - for K^0_S) and the corresponding axis. The acceptance correction was determined using the MC simulation for unpolarised Λ and $\bar{\Lambda}$ decays. The angular dependence of the acceptance is quite smooth, it decreases by a factor 1.2-1.3 in the angular interval used.

To determine the $\Lambda(\bar{\Lambda})$ angular distributions, a sideband subtraction method is used. The events with an invariant mass within a $\pm 1.5\ \sigma$ interval from the mean value of the $\Lambda(\bar{\Lambda})$ peak are taken as signal. The background regions are selected from the left and right sides of the invariant mass peak. Each band is 2 σ wide and starts at a distance of 3 σ from the central value of the peak. The bands of the signal, as well as the background regions, are shown in Fig. 1. The $\Lambda(\bar{\Lambda})$ angular distribution is determined by subtracting the averaged angular distribution of the events in the sidebands from the angular distribution of those in the signal region.

Figure 3 shows the acceptance corrected angular distributions for all events of the 2004 run for Λ and $\bar{\Lambda}$. The events of the 2003 run have similar angular distributions.

3.2 Longitudinal spin transfer

The spin transfer coefficient $D^{\Lambda}_{LL'}$ describes the probability that the polarisation of the struck quark along the primary quantisation axis L is transferred to the Λ hyperon along the secondary quantisation axis L'. In our case the primary and the secondary axes are the same $L = L'$ and coincide with the virtual photon momentum. The longitudinal spin transfer relates the longitudinal polarisation of the hyperon P_L to the polarisation of the incoming lepton beam P_b:

$$P_L = D^{\Lambda}_{LL} \cdot P_b \cdot D(y). \tag{2}$$

The longitudinal polarisation P_L is determined from a fit of the angular distribution (1). The virtual photon depolarisation factor $D(y)$ is given by:

$$D(y) = \frac{1-(1-y)^2}{1+(1-y)^2}. \tag{3}$$

To evaluate the spin transfer, the product $P_b \cdot D(y)$ is calculated for each event passing the selection criteria. The beam polarisation P_b is parametrised as a function of the incident muon momentum [25]. The $P_b \cdot D(y)$ distribution is determined by subtraction of the averaged distribution of the sideband events from the distribution of the events in the signal region, marked by solid lines in Fig. 1. The average value of the $P_b \cdot D(y)$ distribution is used to calculate the D^{Λ}_{LL} according to Eq. (2).

The weighted averages of the spin transfers for the 2003 and the 2004 data are:

$$D^{\Lambda}_{LL} = -0.012 \pm 0.047(stat) \pm 0.024(sys),\ \bar{x}_F = 0.22, \tag{4}$$

$$D^{\bar{\Lambda}}_{LL} = 0.249 \pm 0.056(stat) \pm 0.049(sys),\ \bar{x}_F = 0.20. \tag{5}$$

The systematic errors are mainly due to the uncertainty of the acceptance correction determined by the Monte Carlo simulation. The presence of possible systematic effects was checked by looking at the result of a physical process with no polarisation effects, i.e. the longitudinal spin transfers to the $\mathrm{K}^0_{\mathrm{S}}$ and by checking the stability of the result by varying the selection cuts. The longitudinal spin transfer to the $\mathrm{K}^0_{\mathrm{S}}$ turns out to be $D^{K^0_S}_{LL} = 0.016 \pm 0.010$. The value of the longitudinal spin transfer for kaons is taken as an estimate for the corresponding systematic error $\delta(K^0_S)$. Some systematic effect $\delta(\theta)$ appears due to variation of the cut on $\cos\theta$. The uncertainty of the sidebands subtraction method, $\delta(ss)$ is estimated by varying the width of the central band of Fig. 1 from $\pm 1.5\,\sigma$ to ± 1, ± 1.25, ± 1.75 and $\pm 2\,\sigma$. Another source of systematic errors is the uncertainty in the beam polarisation, $\delta(P_b)$. The relative error in the value of beam polarisation is 0.05.

The values of the systematic errors are given in Table 2. The total systematic error was obtained by summing the various contributions in quadrature.

Table 2: Systematic errors for the spin transfer to Λ and $\bar{\Lambda}$.

	Λ	$\bar{\Lambda}$
Spin transfer to kaons, $\delta(K^0_S)$	0.016	0.016
Variation of the $\cos\theta$ cut, $\delta(\theta)$	0.016	0.044
Uncertainty of the ss-method, $\delta(ss)$	0.010	0.016
Uncertainty of the beam polarisation, $\delta(P_b)$	0.0006	0.013
σ_{syst}	0.024	0.049

3.3 Dependence of the Λ and $\bar{\Lambda}$ spin transfer on x and x_F

The x and x_F dependences of the spin transfers to Λ and $\bar{\Lambda}$ are shown in Figs. 4 and 5. These dependences are different for Λ and $\bar{\Lambda}$. The spin transfer to Λ is small and compatible with zero in the entire x range, while the spin transfer to $\bar{\Lambda}$ may reach values as large as $D^{\bar{\Lambda}}_{LL} = 0.4 - 0.5$.

A similar difference between Λ and $\bar{\Lambda}$ spin transfers is observed in the x_F dependence (Fig. 5). The spin transfer to $\bar{\Lambda}$ tends to increase with x_F, while the Λ one does not show any significant x_F dependence.

4 Discussion of the results

A comparison of the x_F dependence of the longitudinal spin transfer to Λ and $\bar{\Lambda}$ for COMPASS and other experiments [20, 21, 22, 23] is shown in Fig. 6. For Λ there is general agreement between the present results and existing data. For $\bar{\Lambda}$ the measurement of the E665 Collaboration [22] indicated a positive spin transfer (see Fig. 6b). The present result confirms this observation with a much better statistical precision. The NOMAD Collaboration has found [21] that the spin transfer to $\bar{\Lambda}$ is $D_{LL}^{\bar{\Lambda}} = 0.23 \pm 0.15 \pm 0.08$ at $\bar{x}_F = 0.18$ in a good agreement with the present result (5). The measured $D_{LL}^{\bar{\Lambda}}$ increases with x_F, the same trend was found for the Λ polarisation in the experiments at LEP [15, 16].

The main conclusion from the our results is that the longitudinal spin transfers to Λ and $\bar{\Lambda}$ hyperons in DIS are not equal. To understand this phenomenon let us consider the leading order (LO) parton model, where the spin transfer to $\Lambda(\bar{\Lambda})$ produced on an unpolarised target by polarised leptons is given by (see for example [9]):

$$D_{LL}^{\Lambda(\bar{\Lambda})}(x,z) = \frac{\sum_q e_q^2 q(x) \Delta D_q^{\Lambda(\bar{\Lambda})}(z)}{\sum_q e_q^2 q(x) D_q^{\Lambda(\bar{\Lambda})}(z)}. \tag{6}$$

Here e_q is the quark charge, $q(x)$ is the unpolarised quark distribution function, $D_q^{\Lambda(\bar{\Lambda})}(z)$ and $\Delta D_q^{\Lambda(\bar{\Lambda})}(z)$ are the unpolarised and the polarised quark fragmentation functions.

Practically all models of the Λ spin structure predict that the contribution from the s-quark to the Λ spin is dominant. This contribution varies from 100% for the SU(6) model to 60-70% in the BJ-model [3] or the lattice-QCD calculation [28]. It means that scattering off u- or d-quarks is important for the $\Lambda(\bar{\Lambda})$ production but not for the spin transfer to $\Lambda(\bar{\Lambda})$. Accordingly, the polarised fragmentation functions ΔD_s^{Λ} entering in the numerator of Eq. (6) is expected to be much larger than its light quarks counterparts. Therefore, one may assume that $\Delta D_q^{\Lambda}(z) = \Delta D_q^{\bar{\Lambda}}(z) \sim 0$ for $q = u, d, \bar{u}, \bar{d}$. Then the sum in the numerator of (6) is reduced to the strange quark contribution:

$$D_{LL}^{\Lambda}(x,z) \approx \frac{1}{9} \frac{s(x) \Delta D_s^{\Lambda}(z)}{\sum_q e_q^2 q(x) D_q^{\Lambda}(z)}, \tag{7}$$

$$D_{LL}^{\bar{\Lambda}}(x,z) \approx \frac{1}{9} \frac{\bar{s}(x) \Delta D_{\bar{s}}^{\bar{\Lambda}}(z)}{\sum_q e_q^2 q(x) D_q^{\bar{\Lambda}}(z)}. \tag{8}$$

From (7)-(8) it is seen that the spin transfer from the polarised lepton to Λ and $\bar{\Lambda}$ must be different even if $s(x) = \bar{s}(x)$. The reason is that the denominators of (7) and (8) are proportional to the $\Lambda(\bar{\Lambda})$ production cross section. Due to the combined effect of the u-quark dominance and the favoured fragmentation of u-quark to Λ, as opposed to $\bar{\Lambda}$, the cross section for Λ is expected to be larger. This expectation is confirmed by the measured yields of Λ and $\bar{\Lambda}$, reported in Sect. 2. Therefore, one may expect a smaller spin transfer to Λ than to $\bar{\Lambda}$.

This conclusion of the LO parton model has been confirmed by the calculation of [2], shown in Figs. 4,5. The model is based on the LEPTO [26] MC event generator, in which the independent fragmentation is replaced by the hadronisation of the string formed by the struck quark and the target remnant. All contributions, including those from the target remnant and from decays of heavy hyperons are taken into account. Figs. 4,5 show that indeed calculations of the model [2] lead to a larger spin transfer to $\bar{\Lambda}$ than to Λ. The same trend was found in the recent calculation of [12].

Another indication from the parton model Eqs. (7)-(8) is that the contribution from the strange quarks (antiquarks) is essential for the spin transfer to $\Lambda(\bar{\Lambda})$. This observation is also confirmed by the results of [2]. In Fig. 7 the degree of the sensitivity to the strange parton distributions is illustrated by the comparison of the results obtained with the CTEQ5L [29](solid line) and GRV98LO [30](dashed line) parton distributions. The GRV98 set is chosen because of its assumption that there is no intrinsic nucleon strangeness at a low scale and the strange sea is of pure perturbative origin. The CTEQ Collaboration allows non-perturbative strangeness in the nucleon. The amount of this intrinsic strangeness is fixed from the dimuon data of the CCFR and NuTeV experiments [31]. As a result, the $s(x)$ distribution of CTEQ is larger than the GRV98 one by a factor of about two in the region $x = 0.001 - 0.01$. The results in Fig. 7 show that the data on Λ can not discriminate between the predictions since the spin transfer to Λ is small. For the $\bar{\Lambda}$ hyperon the use of CTEQ5L set leads to a prediction which is nearly twice larger than the one with the GRV98LO and much closer to the data. This behaviour reflects the difference in the corresponding $\bar{s}$-quark distributions. If one completely switches off the spin transfer from the $s(\bar{s})$ quarks, the spin transfer to $\Lambda(\bar{\Lambda})$ practically vanishes (dash-dotted line). This feature is independent of

the model of Λ spin structure. Calculations in the BJ-model [3], where the spin transfer from the u- and d-quarks(antiquarks) is possible, demonstrate the same absence of the spin transfer to hyperon without contribution from the $s(\bar{s})$-quarks (dotted line).

At present the strange and antistrange quark distributions $s(x)$ and $\bar{s}(x)$ are directly accessible only through the measurement and study of dimuon events in neutrino and antineutrino DIS [32]. The spin transfer to $\bar{\Lambda}$ could provide an additional experimental information for determination of strange quark distributions in the nucleon. To match this goal the present experimental precision must be increased and the theoretical uncertainties should be clarified. For instance, the parameters of the model [2] have been fixed by fitting the NOMAD data [20] at comparatively large x and its predictions can be considered as an illustration of the possible effects.

5 Conclusions

The longitudinal polarisation transfer from polarised muons to semi-inclusively produced Λ and $\bar{\Lambda}$ hyperons has been studied in deep-inelastic scattering at the COMPASS experiment. The present data are the most precise measurements to date of the longitudinal spin transfer to Λ and $\bar{\Lambda}$ in DIS. The results show that the spin transfer to Λ is small with $D_{LL}^{\Lambda} = -0.012 \pm 0.047 \pm 0.024$ at $\bar{x}_F = 0.22$. The spin transfer to $\bar{\Lambda}$ is larger with $D_{LL}^{\bar{\Lambda}} = 0.249 \pm 0.056 \pm 0.049$ at $\bar{x}_F = 0.20$. These values are in agreement with results of previous measurements [20, 21, 22, 23].

We have also measured the x and x_F dependences of the longitudinal spin transfer which are different for Λ and $\bar{\Lambda}$ hyperons. The spin transfer to Λ is small, compatible with zero, in the entire domain of the measured kinematic variables. In contrast, the longitudinal spin transfer to $\bar{\Lambda}$ increases with x_F reaching values of $D_{LL}^{\Lambda} = 0.4 - 0.5$. Comparison with theory shows that the spin transfer to the $\bar{\Lambda}$ hyperon strongly depends on the antistrange quark distribution $\bar{s}(x)$ and therefore the precise measurements of the $\bar{\Lambda}$ spin transfer will provide useful information about the antistrange quark distribution $\bar{s}(x)$.

Acknowledgement

We gratefully acknowledge the support of the CERN management and staff, the skill and effort of the technicians of our collaborating institutes. Special thanks are due to V. Anosov and V. Pesaro for their technical support during installation and running of this experiment. It is a pleasure to thank J. Ellis, Liang Zuo-tang, D. Naumov and S. Belostotsky for stimulating discussions.

References

[1] J. Ellis, A. M. Kotzinian, D. Naumov, *Eur. Phys. J.* **C25** (2002) 603.
[2] J. Ellis, A. M. Kotzinian, D. Naumov, M. G. Sapozhnikov, *Eur. Phys. J.* **C52** (2007) 283.
[3] M. Burkardt, R. L. Jaffe, *Phys. Rev. Lett.* **70** (1993) 2537.
[4] I. I. Bigi, *Nuov. Cim.* **41A** (1977) 43.
[5] G. Gustafson, J. Hakkinen, *Phys. Lett.* **B303** (1993) 350.
[6] M. Anselmino, M. Boglione and F. Murgia, *Phys. Lett.* **B481** (2000) 253.
[7] D. Ashery, H. J. Lipkin, *Phys. Lett.* **B469** (1999) 263–269.
[8] D.de Florian, M. Stratmann, W. Vogelsang, *Phys. Rev.* **D57** (1998) 5811.
[9] A. M. Kotzinian, A. Bravar and D. von Harrach, *Eur. Phys. J.* **C2** (1998) 329.
[10] Dong Hui, Zhou Jian, Liang Zuo-tang, *Phys. Rev.* **D72** (2005) 033006.
[11] Q. Xu, Liang Zuo-tang, E. Sichtermann, *Phys. Rev.* **D73** (2006) 077503.
[12] Liang Zuo-tang et al. (2009), hep-ph/0902.1883.
[13] B. Ma, I. Schmidt, J. Soffer, J. Yang, *Phys. Lett.* **B488** (2000) 254–260.
[14] B. Ma, I. Schmidt, J. Yang, *Phys. Lett.* **B477** (2000) 107.
[15] ALEPH Collaboration, D. Buskulic et al., *Phys. Lett.* **B374** (1996) 319.
[16] OPAL Collaboration, K. Ackerstaff et al., *Eur. Phys. J.* **C2** (1998) 49.
[17] WA21 Collaboration, G. T. Jones et al., *Z. Phys.* **C28** (1985) 23.
[18] WA59 Collaboration, S. Willocq et al. , *Z. Phys.* **C53** (1992) 207.
[19] E632 Collaboration, D. De Prospo et al., *Phys. Rev.* **D50** (1994) 6691.
[20] NOMAD Collaboration, P. Astier et al., *Nucl. Phys.* **B588** (2000) 3.
[21] NOMAD Collaboration, P. Astier et al., *Nucl. Phys.* **B605** (2001) 3.
[22] E665 Collaboration, M. R. Adams et al., *Eur. Phys. J.* **C17** (2000) 263.
[23] HERMES Collaboration, A. Airapetian et al., *Phys. Rev.* **D74** (2006) 072004.
[24] STAR Collaboration, Quinhua Xu, *Proc.17th International Spin Physics Symposium (SPIN06), Kyoto, AIP conference Proceedings,* **915** (2006) 428, hep-ex/0612035.
[25] COMPASS Collaboration, P. Abbon et al., *Nucl. Instrum. Meth.* **A577** (2007) 455.
[26] G. Ingelman, A. Edin, J. Rathsman, *Comp. Phys. Commun.* **101** (1997) 108.

[27] T. Sjöstrand, *Comp. Phys. Commun.* **82** (1994) 74.
[28] M. Göckeler et al., *Phys. Lett.* **B545** (2002) 112.
[29] F. Olness et al., *Eur. Phys. J.* **C 40** (2005) 145.
[30] M. Glück, E. Reya, A. Vogt, *Eur. Phys. J.* **C5** (1998) 461.
[31] CCFR and NuTeV Collaborations, M. Goncharov et al., *Phys. Rev.* **D64** (2001) 112006.
[32] D. Mason et al., *Phys. Rev. Lett.* **99** (2007) 192001.

Figures

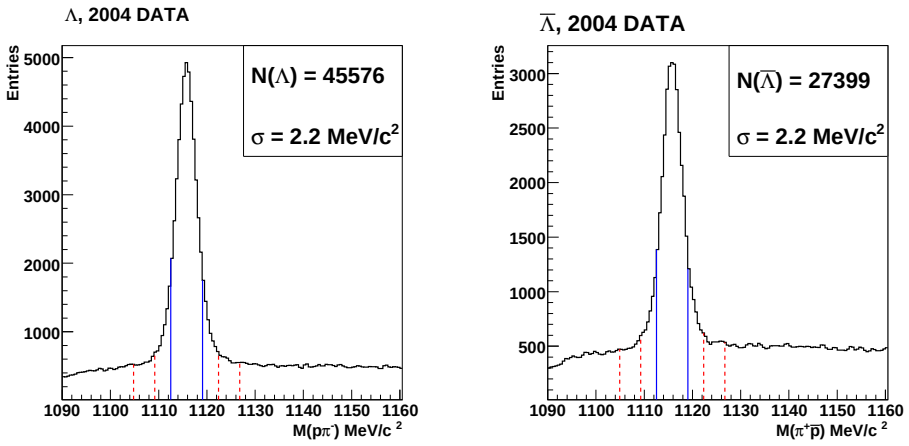

a) b)

Figure 1: The invariant mass distribution for the $p\pi^-$ (a) and $\bar{p}\pi^+$ (b) hypothesis for the data of 2004 run. The solid lines marks the band of the $\Lambda(\bar{\Lambda})$ signal, the dashed lines show the sidebands used for determination of the background regions.

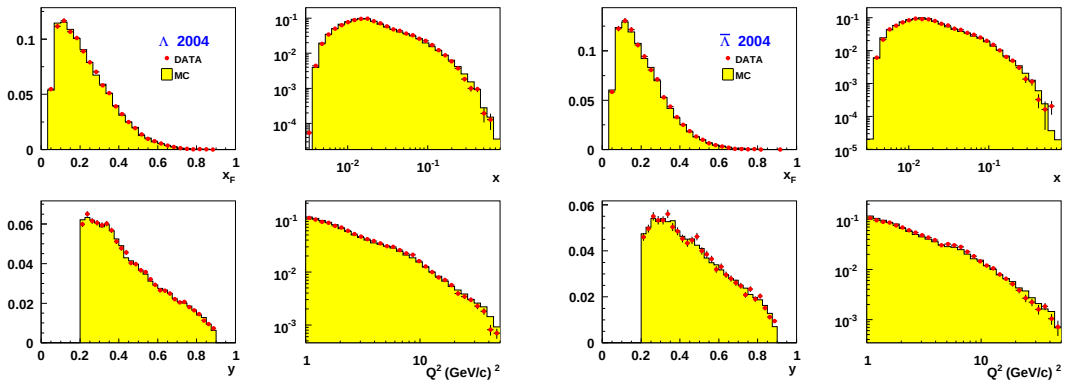

a) b)

Figure 2: Comparison between the experimental data (circles) and MC (histograms) on x_F, x, y and Q^2 distributions of the Λ (a) and $\bar{\Lambda}$ (b) hyperons. The data are for the 2004 run.

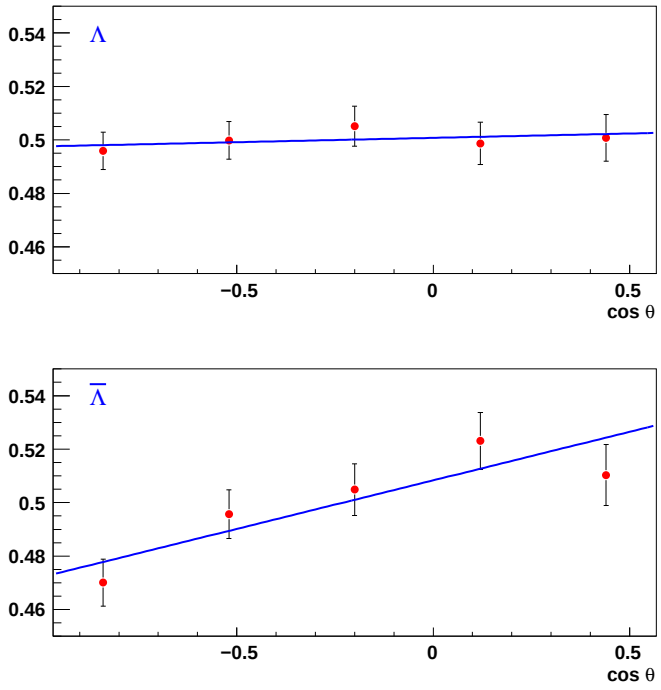

Figure 3: The normalised angular distributions, corrected for acceptance, for the Λ and $\bar{\Lambda}$ for all events of the 2004 run. The solid line is the result of the linear fit to Eq. (1).

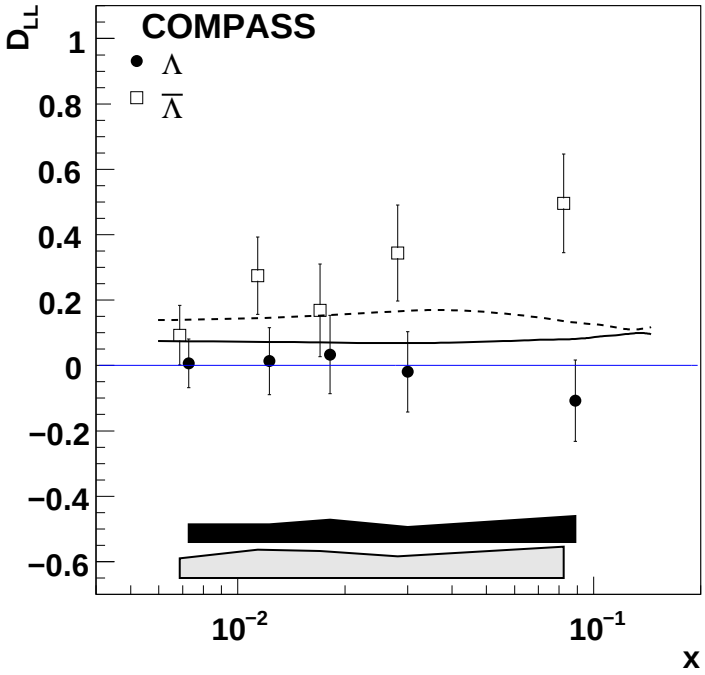

Figure 4: The x dependence of the longitudinal spin transfer to Λ and $\bar{\Lambda}$. The solid line corresponds to the theoretical calculations of [2](Model B, SU(6),CTEQ5L) for Λ and the dashed line is for the $\bar{\Lambda}$ spin transfer.The shaded bands show the size of the corresponding systematic errors.

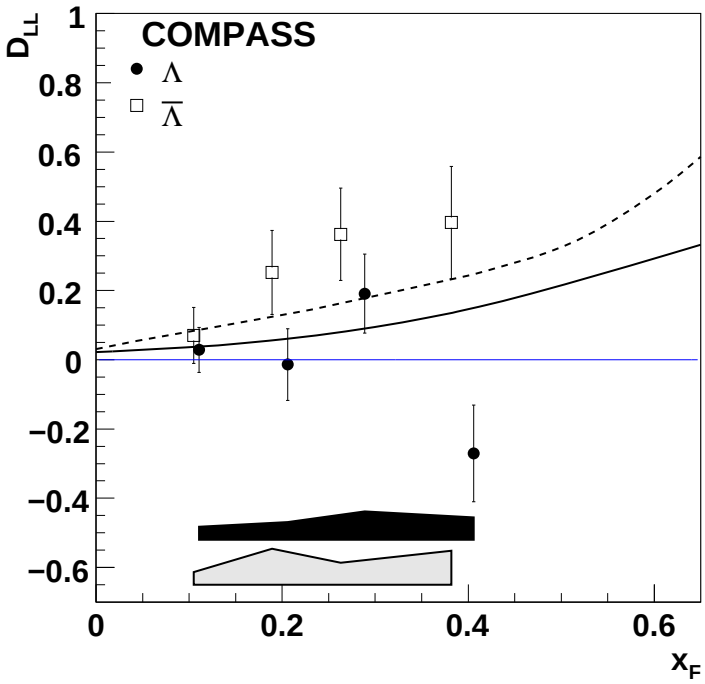

Figure 5: The x_F dependence of the longitudinal spin transfer to Λ and $\bar{\Lambda}$. The solid line corresponds to the theoretical calculations of [2](Model B, SU(6),CTEQ5L) for Λ and the dashed line is for the $\bar{\Lambda}$ spin transfer. The shaded bands show the size of the corresponding systematic errors.

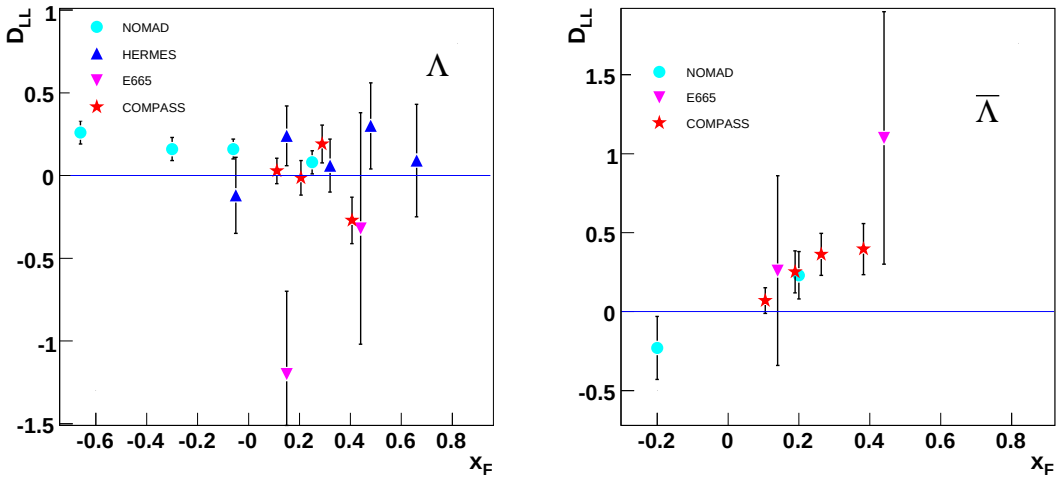

a) b)

Figure 6: The x_F dependence of the longitudinal spin transfer to Λ (a) and $\bar{\Lambda}$ (b) for the COMPASS (stars) and other experiments [20, 21, 22, 23](NOMAD data- circles, E665 - reverse triangles, HERMES - triangles).

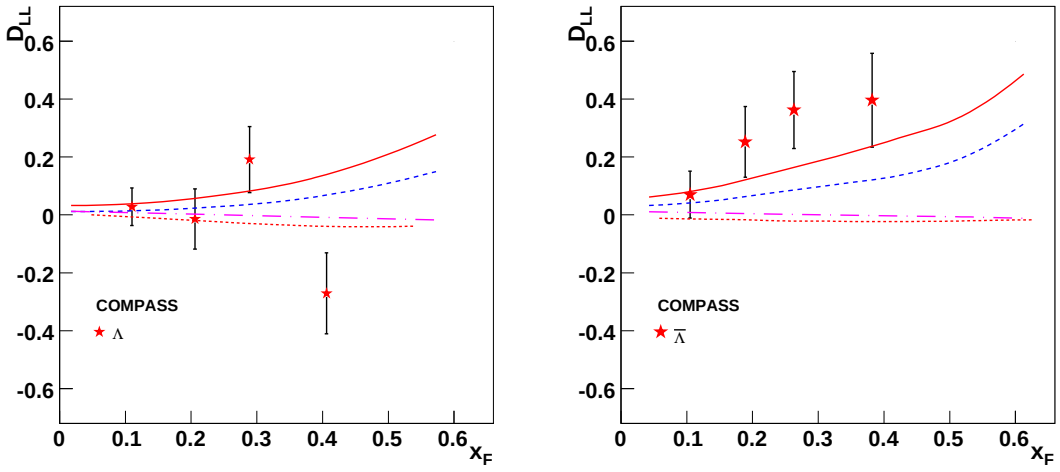

a) b)

Figure 7: The x_F dependences of the longitudinal spin transfer to Λ (a) and $\bar{\Lambda}$ (b) calculated in [2](model B) for the GRV98LO parton distribution functions (dashed lines), the CTEQ5L pdf (solid lines) and for the CTEQ5L without spin transfer from the s-quark (dash-dotted lines). The SU(6) model for the Λ spin structure is assumed. The dotted lines corresponds to the calculations for the CTEQ5L without spin transfer from the s-quark in the BJ-model of Λ spin [3].